Accelerating high-fidelity combustion simulations with classification algorithms

Wai Tong Chung,[1,*] **Aashwin Ananda Mishra,** [2] **Nikolaos Perakis,** [1,3] **Matthias Ihme,** [1]

[1] Department of Mechanical Engineering, Stanford University, Stanford, CA 94305, USA
[2] SLAC National Accelerator Laboratory, Menlo Park, CA 94025, USA
[3] Chair of Space Propulsion, Technical University of Munich, 85748 Garching, Germany
[*] Corresponding author: wtchung@stanford.edu

Abstract

High-fidelity combustion simulations are useful for optimizing engineering designs, and can result in reduced design costs, increased engineering performance, and lower emissions. In these simulations, the representation of combustion chemistry is a computational bottleneck. In this investigation, we accelerate unsteady combustion simulations by employing neural networks for dynamic combustion submodel assignment. Neural networks, trained with local flow properties as input variables and combustion model errors as training labels, assign three different combustion models – finite-rate chemistry (FRC), flamelet progress variable (FPV), and inert mixing (IM) – with high classification accuracy in *a priori* tests. *A priori* results are compared with those generated by random forests. *A posteriori* simulations, integrating a neural network model in the computational fluid dynamics solver, demonstrate that high-fidelity simulations can be performed with this approach at significantly reduced cost compared to detailed chemistry simulations and simultaneously achieving improved accuracy over low-order combustion models.

Introduction

Combustion processes are present in engineering applications, such as in rockets, thermal generators, and propulsion engines. Thus, accurate combustion simulation techniques are useful for optimizing engineering designs, and can result in reduced design costs, increased engineering performance, and substantially lower greenhouse-gas emissions and pollutants. However, commonplace adoption of such high-fidelity simulation techniques is restricted by a bottleneck that emerges from the high computational expense of combustion chemistry. Hence, a significant portion of combustion research has been devoted to the development of cost-efficient models for representing the combustion chemistry (Pope 2013) in large-scale high-fidelity simulations.

Alternatively, data-driven methods can be employed for fast and accurate predictive modeling. In particular, artificial neural networks have been employed for regressing thermophysical quantities (Christo et al. 1996; Blasco et al. 1999; Ihme, Schmitt, and Pitsch 2009; Kempf, Flemming, and Janicka 2005; Sen and Menon 2010), and modeling turbulent

terms (Lapeyre et al. 2019; Henry de Frahan et al. 2019). However, supervised learning in flow-physics problems are still in their infancy, and face challenges when extrapolating beyond the training set – resulting in generalization errors that arise from numerical predictions that only match specific flow configurations represented by the training data (Wu, Xiao, and Paterson 2018).

This study ameliorates this issue by employing a machine learning classification algorithm that selects well-tested physics-based combustion submodels of varying fidelity and complexity, and assigns them to different regions of the simulation domain. Thus, the potential approximation errors made by the machine-learning algorithm are limited by the predictive capability of the lowest performing submodel. Previous work (Chung et al. 2020) has investigated the use of random forests (Breiman 2001) for combustion submodel assignment. While random forests can provide high classification accuracy, the development of deep learning methods provides advantages to neural networks in learning spatial and temporal data, commonly seen in flow-physics problems.

To this end, we examine the application of employing neural networks for the purpose of local and dynamic model assignment in large-eddy simulations (LES) of a gaseous-oxygen/gaseous-methane (GOX/GCH4) rocket combustor (Silvestri et al. 2015, 2016). Results from an *a priori* investigation are assesed and compared with results from random foretts. Additionally, an *a posteriori* neural network-integrated simulation to demonstrate the effectiveness of this approach, and the computational gains achieved.

Mathematical models

Large-eddy simulations in the present study are performed by solving the Favre-filtered conservation equations for mass, momentum, energy, and chemical species:

$$\partial_t \overline{\rho} + \nabla \cdot (\overline{\rho}\widetilde{\boldsymbol{u}}) = 0 \tag{1a}$$

$$\partial_t(\overline{\rho}\widetilde{\boldsymbol{u}}) + \nabla \cdot (\overline{\rho}\widetilde{\boldsymbol{u}}\widetilde{\boldsymbol{u}}) = -\nabla \cdot (\overline{p}\boldsymbol{I}) \\ + \nabla \cdot (\overline{\boldsymbol{\tau}}_v + \boldsymbol{\tau}_t) \tag{1b}$$

$$\partial_t(\overline{\rho}\widetilde{e}) + \nabla \cdot [\widetilde{\boldsymbol{u}}(\overline{\rho}\widetilde{e} + \overline{p})] = -\nabla \cdot (\overline{\boldsymbol{q}}_v + \boldsymbol{q}_t) \\ + \nabla \cdot [(\overline{\boldsymbol{\tau}}_v + \boldsymbol{\tau}_t) \cdot \widetilde{\boldsymbol{u}}] \tag{1c}$$

$$\partial_t(\overline{\rho}\widetilde{\phi}) + \nabla \cdot (\overline{\rho}\widetilde{\boldsymbol{u}}\widetilde{\phi}) = -\nabla \cdot (\overline{\boldsymbol{J}}_v + \boldsymbol{J}_t) + \dot{\overline{\boldsymbol{S}}} \tag{1d}$$

with density ρ, velocity vector $\boldsymbol{u}$, specific total energy e, stress tensor $\boldsymbol{\tau}$, and heat flux vector $\boldsymbol{q}$; $\overline{}$ denotes a filtered

quantity and $\widetilde{\cdot}$ is a Favre-filtered quantity. Subscripts v and t denote viscous and turbulent quantities, respectively. The pressure p is computed from the ideal gas equation of state. $\boldsymbol{\phi}$, $\boldsymbol{J}$, and $\dot{\boldsymbol{S}}$ are the transported scalars, scalar diffusive fluxes, and scalar source terms for the candidate combustion models. The dynamic Smagorinsky model (Moin et al. 1991) and dynamic thickened-flame model (Colin et al. 2000) are used to model closure in the turbulent terms. Simulations are performed by employing an unstructured compressible finite-volume solver (Khalighi et al. 2011; Ma, Lv, and Ihme 2017; Wu et al. 2019).

In this work, we employ three different combustion submodels, namely an inert mixing (IM) model, the flamelet/progress variable (FPV) model (Pierce and Moin 2004; Ihme, Cha, and Pitsch 2005), and a finite-rate chemistry (FRC) model. The present framework couples the different combustion models with the approach developed by Wu et al. (2019), which ensures the conservation of mass, momentum, and energy. Reconstruction of the chemical state-vector needed for FRC involves interpolation from the chemistry tables that stores all species, whereas the reconstruction of the progress variable needed for tabulated chemistry involves the sum of all major combustion product species: CO_2, CO, H_2O, and H_2. To ensure consistency between the combustion submodels, the aforementioned reconstruction is applied for the inactive combustion model at the submodel interface at every timestep. The GRI-3.0 chemical mechanism (Smith et al. 2000), involving 33 chemical species, is used to describe combustion chemistry.

Experimental configuration and computational setup

We perform simulations of the gaseous oxygen-gaseous methane rocket combustor setup by Silvestri et al. (2015, 2016) using an axisymmetric domain. We select this configuration to challenge the shortcomings of FPV in representing correct wall heat flux, which results in a thicker thermal boundary layer and overprediction of CO mass fraction shown in fig. 1.

Inlet fuel and oxidizer mass flow rates and temperature, along with chamber and nozzle wall temperatures are prescribed following experimental measurements (Silvestri et al. 2015, 2016; Perakis and Haidn 2019). All remaining boundaries are defined as adiabatic non-slip walls with the exception of the exhaust, which is modeled as a pressure outlet. The computational domain is discretized by a block-structured mesh consisting of 2×10^5 cells. The wall-normal direction is resolved down to 30 μm, and a wall model (Kawai and Larsson 2013) is employed for the viscous sublayer. A typical timestep is 25 ns, corresponding to a convective CFL number of 1.0.

Data-driven methods

In this section, we describe the procedure for incorporating a supervised learning algorithm for combustion submodel assignment. Firstly, we use the instantaneous flow-field solutions from the FRC simulation of the combustor as the learning dataset. FRC data are then used to reconstruct FPV

and IM quantities of interest Q by interpolating from generated flamelet tables (Pitsch 1998).

Secondly, we assign labels $\mathcal{Y} = \{$IM, FPV, FRC$\}$ to the training data. We consider FRC as combustion model of highest fidelity but at the expense of highest computational cost. Therefore, we assign labels in the training set based on the normalized combustion submodel error ϵ_Q^y of quantities of interest $\alpha \in Q$ between FRC and the models of lower fidelity (Wu et al. 2015):

$$\epsilon_Q^y = \frac{1}{N} \sum_{\alpha \in Q} \frac{|\alpha^{\text{FRC}} - \alpha^y|}{\|\alpha^{\text{FRC}}\|_\infty} \text{ with } y \in \{\text{FPV}, \text{IM}\}, \quad (2)$$

where the error for considering $N = |Q|$ number of quantities of interest (QoIs) is a normalized linear combination of each individual submodel error. A model of higher fidelity is assigned when the QoI submodel error ϵ_Q^y exceeds a user-defined threshold θ_Q^y, with FRC chosen when all conditions for selecting FPV and IM are not met.

Thirdly, we construct the feature vector $\boldsymbol{x} \in \mathcal{X}$. To this end, we applied the Maximal Information Coefficient (MIC) (Reshef et al. 2011) to identify the top six (out of fifteen) thermophysical quantities with the strongest relationships with the local combustion submodel error. These six features, namely mixture fraction, progress variable, density, local Prandtl number, and Euclidean norm of the mixture fraction gradient, *viz.,* $\boldsymbol{x} = [\widetilde{Z}, \widetilde{C}, \overline{\rho}, \widetilde{T}, Pr_\Delta, \|\nabla \widetilde{Z}\|_2]$ are then selected for constructing the feature set.

Lastly, we train, validate, and test the classification algorithms. In this investigation, we compare the combustion submodel assignment by neural networks and random forests in the *a priori* study. 1×10^4 training points have been randomly sampled from a single simulation snapshot consisting of 2×10^5 cells. The hyperparameters of a random forest, consisting of twenty decision trees, and maximum depth of ten nodes, are found using random grid search. Addtionally, the hyperparameters of a neural network consisting of 4 hidden dense layers with L2 regularization consisting of 36 nodes are found using Bayesian optimization.

Results

We first perform an *a priori* assessment to determine the accuracy of neural network and random forest classification, as shown in Table 1, on a monolithic FRC simulation test dataset from an unseen timestep. Temperature and CO mass fraction fields from the test dataset are shown in fig. 2a. and 2b. Temperature $\widetilde{T}$ is chosen as a QoI to describe the combustion efficiency and engine performance. CO mass fraction, $\widetilde{Y}_{\text{CO}}$, is chosen to challenge the deficiencies of FPV and IM in capturing intermediate species (Wu et al. 2019). Throughout this study we explore cases that use the same threshold for both IM and FPV, *viz.,* $\theta_Q^{\text{IM}} = \theta_Q^{\text{FPV}} = \theta_Q$ for simplicity. Classification accuracy range from approximately 0.7 to 0.8, which is comparable to the use of classifiers in other flow physics problems (Maulik et al. 2019). We note that while the combustion submodel assignment accuracy of both classifiers are comparable, neural networks produce less 'speckled' submodel assignment. This is an improvement as it reduces the
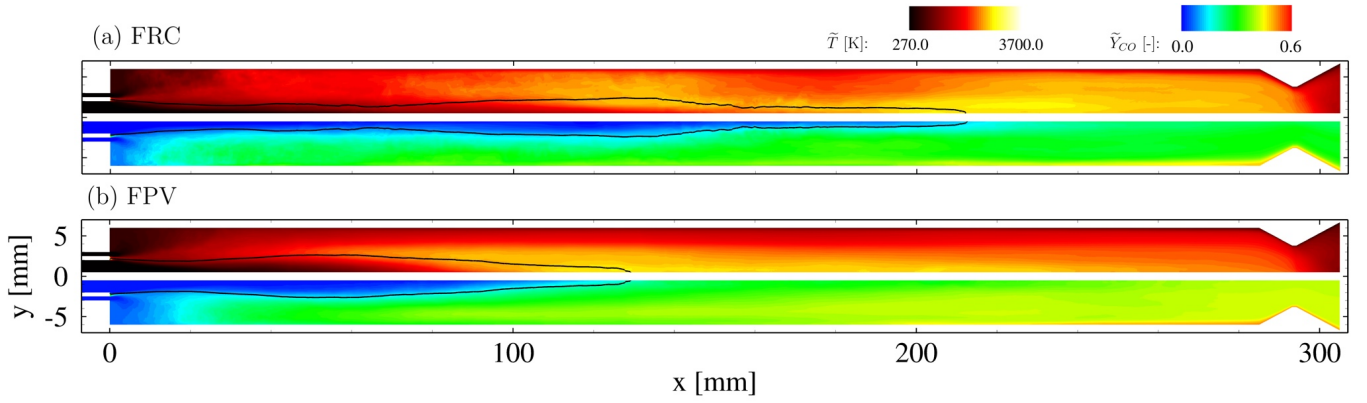
Figure 1: Time-averaged temperature and CO mass fraction for monolithic FRC and FPV LES. The location of the stoichiometric mixture, $\widetilde{Z}_{st} = 0.2$, is shown by black lines.

Table 1: *A priori* analysis of neural networks, summarizing submodel assignment and assignment accuracy.

Case	$\theta_{\{T,\mathrm{CO}\}}=0.05$	$\theta_{\{T,\mathrm{CO}\}}=0.02$	$\theta_{\{T,\mathrm{CO}\}}=0.05$	$\theta_{\{T,\mathrm{CO}\}}=0.02$
Classifier	Neural network	Neural network	Random forest	Random forest
IM:FPV:FRC	6:74:20	5:46:49	6:63:31	6:42:52
Classification accuracy	0.773	0.696	0.753	0.734
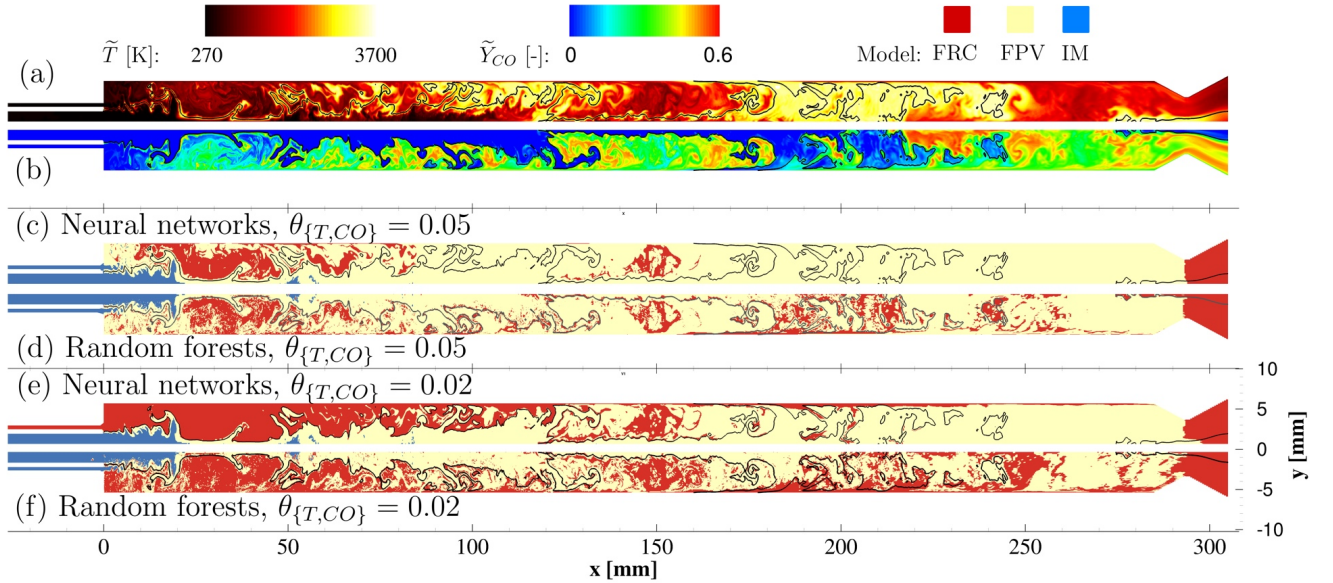
Figure 2: Instantaneous (a) temperature, (b) CO mass fraction, and (c,d) combustion submodel assignment from test set in the *a priori* assessment. The location of the stoichiometric mixture, $\widetilde{Z}_{st} = 0.2$, is shown by black lines.

reconstruction operations between the different combustion submodels at the submodel interface.

Figure 2c. and 2d. demonstrates the *a priori* combustion submodel assignment on an unseen FRC-simulation snapshot for case $\theta_{\{T,\mathrm{CO}\}} = 0.05$ using a neural network and random forest respectively. For both cases shown, inert mixing (IM) is assigned in 6% of the domain at the injector and the oxidizer core, where chemical processes are insignificant. In general,

FRC is assigned in fuel-rich regions immediately downstream of the injectors where intermediate species reactions are not captured well by tabulated chemistry submodels. Employing random forest results in 31% FRC assignment within the domain, while neural network results 20% FRC assignment.

Figure 2e. and 2f. demonstrates the *a priori* combustion submodel assignment for case $\theta_{\{T,\mathrm{CO}\}} = 0.02$ using a neural network and random forest respectively. Here, the neural
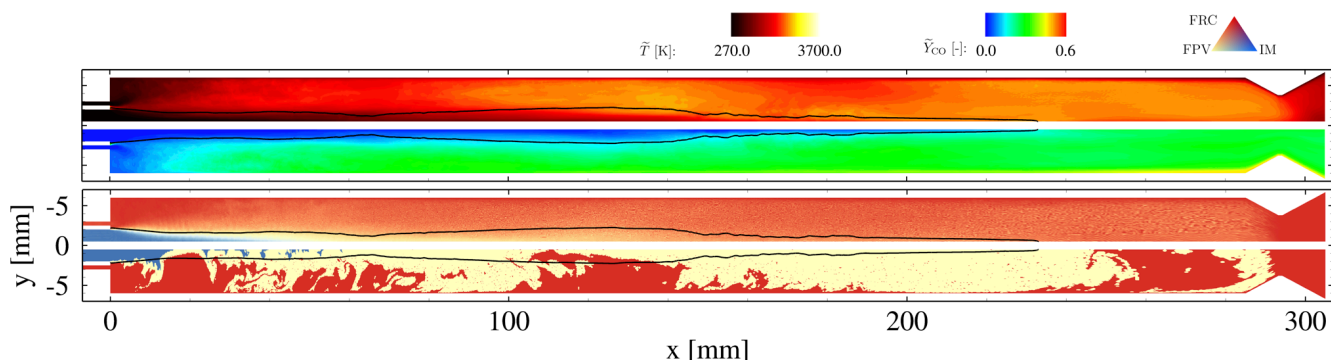
Figure 3: Time-averaged temperature, CO mass fraction, along with time-averaged and instantaneous combustion submodel assignment for *a posteriori* data-assisted LES using neural-networks. The location of the stoichiometric mixture, $\widetilde{Z}_{st} = 0.2$, is shown by black lines.

network fails to recognize that IM should be applied to the fuel injector, resulting in a lower overall IM assignment of 5%. In addition to the aforementioned fuel rich region, both classifiers assign FRC to the near wall regions, which are essential for accurate thermal and species boundary layer predictions. This results in 49% and 52% FRC assignment for the neural network and random forest respectively.

Figure 3 shows temperature and CO mass fraction fields from an *a posteriori* data-assisted (DA) LES, using model threshold $\theta_{\{T,\text{CO}\}} = 0.02$, performed by employing a neural network classifier in-flight for combustion submodel assignment during simulation runtime. Temperature and CO mass fraction fields are in good agreement with the monolithic FRC LES in fig. 1, with thermal boundary layer and CO mass fraction captured correctly. The corresponding combustion submodel assignment is also shown in fig. 3. FRC utilization is at 66%, resulting in 75% FRC cost, or – equivalently – a reduction in the computational cost by 25%.

Conclusions

This work demonstrates a data-driven modeling approach by which neural network and random forest classifiers spatially and dynamically assign three different candidate combustion submodels. This modeling approach is demonstrated in simulations of a complex rocket combustor. Results demonstrated that neural networks and random forests showed high classification accuracy for this task. However, random forests produce more speckled submodel assignment than neural networks. *A posteriori* simulations incorporating neural networks showed significant improvements from monolithic FPV simulations in all quantities at a *25% lower cost* than monolithic FRC calculations. Interesting opportunities for extending this work include the exploration of convolutional and recurrent layers in neural networks to better incorporate spatial and temporal data.

Acknowledgments

References

Blasco, J. A.; Fueyo, N.; Larroya, J. C.; Dopazo, C.; and Chen, J. Y. 1999. Single-step time-integrator of a methane-air chemical system using artificial neural networks. *Comput. Chem. Eng.* 23(9): 1127–1133.

Breiman, L. 2001. Random forests. *Mach. Learn.* 45(1): 5–32.

Christo, F. C.; Masri, A. R.; Nebot, E. M.; and Pope, S. B. 1996. An integrated PDF/neural network approach for simulating turbulent reacting systems. *Proc. Combust. Inst.* 26: 43–48.

Chung, W. T.; Mishra, A. A.; Perakis, N.; and Ihme, M. 2020. Data-assisted combustion simulations with dynamic submodel assignment using random forests. *arXiv* 2009.04023.

Colin, O.; Ducros, F.; Veynante, D.; and Poinsot, T. 2000. A thickened flame model for large eddy simulations of turbulent premixed combustion. *Phys. Fluids* 12(7): 1843–1863.

Henry de Frahan, M. T.; Yellapantula, S.; King, R.; Day, M. S.; and Grout, R. W. 2019. Deep learning for presumed probability density function models. *Combust. Flame* 208: 436–450.

Ihme, M.; Cha, C. M.; and Pitsch, H. 2005. Prediction of local extinction and re-ignition effects in non-premixed turbulent combustion using a flamelet/progress variable approach. *Proc. Combust. Inst.* 30: 793–800.

Ihme, M.; Schmitt, C.; and Pitsch, H. 2009. Optimal artificial neural networks and tabulation methods for chemistry representation in les of a bluff-body swirl-stabilized flame. *Proc. Combust. Inst.* 32: 1527–1535.

Kawai, S.; and Larsson, J. 2013. Dynamic non-equilibrium wall-modeling for large eddy simulation at high Reynolds numbers. *Phys. Fluids* 25(1): 015105.

Kempf, A.; Flemming, F.; and Janicka, J. 2005. Investigation of lengthscales, scalar dissipation, and flame orientation in a piloted diffusion flame by LES. *Proc. Combust. Inst.* 30: 557–565.

Khalighi, Y.; Nichols, J. W.; Ham, F.; Lele, S. K.; and Moin, P. 2011. Unstructured large eddy simulation for prediction of noise issued from turbulent jets in various configurations. *AIAA Paper 2011-2886* .

Lapeyre, C. J.; Misdariis, A.; Cazard, N.; Veynante, D.; and Poinsot, T. 2019. Training convolutional neural networks to estimate turbulent sub-grid scale reaction rates. *Combust. Flame* 203: 255–264.

Ma, P. C.; Lv, Y.; and Ihme, M. 2017. An entropy-stable hybrid scheme for simulations of transcritical real-fluid flows. *J. Comput. Phys.* 340: 330–357.

Maulik, R.; San, O.; Jacob, J. D.; and Crick, C. 2019. Subgrid scale model classification and blending through deep learning. *J. Fluid Mech.* 870: 784–812.

Moin, P.; Squires, K.; Cabot, W.; and Lee, S. 1991. A dynamic subgrid-scale model for compressible turbulence and scalar transport. *Phys. Fluids A* 3(11): 2746–2757.

Perakis, N.; and Haidn, O. J. 2019. Inverse heat transfer method applied to capacitively cooled rocket thrust chambers. *Int. J. Heat Mass Transf.* 150–166.

Pierce, C. D.; and Moin, P. 2004. Progress-variable approach for large-eddy simulation of non-premixed turbulent combustion. *J. Fluid Mech.* 504: 73–97.

Pitsch, H. 1998. FLAMEMASTER v3.1: A C++ computer program for 0D combustion and 1D laminar flame calculations.

Pope, S. B. 2013. Small scales, many species and the manifold challenges of turbulent combustion. *Proc. Combust. Inst.* 34: 1–31.

Reshef, D. N.; Reshef, Y. A.; Finucane, H. K.; Grossman, S. R.; McVean, G.; Turnbaugh, P. J.; Lander, E. S.; Mitzenmacher, M.; and Sabeti, P. C. 2011. Detecting novel associations in large data sets. *Science* 334(6062): 1518–1524.

Sen, B. A.; and Menon, S. 2010. Linear eddy mixing based tabulation and artificial neural networks for large eddy simulations of turbulent flames. *Combust. Flame* 157(1): 62–74.

Silvestri, S.; Celano, M. P.; Haidn, O. J.; and Knab, O. 2015. Comparison of single element rocket combustion chambers with round an square cross sections. *6th Euro. Conf. Aeronautics Space Sci. (EUCASS)* .

Silvestri, S.; Celano, M. P.; Kirchberger, C.; Schlieben, G.; Haidn, O.; and Knab, O. 2016. Investigation on recess variation of a shear coax injector for a single element GOX-GCH4 combustion chamber. *Trans. JSASS Aerospace Tech. Japan* 14(ists30): 101–108.

Smith, G. P.; Golden, D. M.; Frenklach, M.; and Moriarty et. al., N. W. 2000. GRI-Mech 3.0. http://www.me.berkeley.edu/gri-mech/.

Wu, H.; Ma, P. C.; Jaravel, T.; and Ihme, M. 2019. Pareto-efficient combustion modeling for improved CO-emission prediction in LES of a piloted turbulent dimethyl ether jet flame. *Proc. Combust. Inst.* 37(2): 2267–2276.

Wu, H.; See, Y. C.; Wang, Q.; and Ihme, M. 2015. A Pareto-efficient combustion framework with submodel assignment for predicting complex flame configurations. *Combust. Flame* 162: 4208–4230.

Wu, J.-L.; Xiao, H.; and Paterson, E. 2018. Physics-informed machine learning approach for augmenting turbulence models: A comprehensive framework. *Phys. Rev. Fluids* 3: 74602.